High Frequency Pulse Width Modulation Converters

Ahmed Hassan Mohammed
Tikrit University / Electrical Engineering Department
ah-a123@yahoo.com
Received date: 29/3/2011 Accepted date: 3/11/2013

Abstract

The delta modulation technique permits an accurate of an arbitrary reference. Spectrum of the current going through an inductive load shows a very low THD. Moreover, notches are located around the sample frequency multiples, which is of interest for converters without output low-pass filter. In this paper, we demonstrate that the delta modulator structure can be easily implemented when regulating the converter output current going through an inductive load. Then, we propose a mean for computing the load current spectrum using the Laplace and Fourier transforms.

Keywords Modulation strategies, converter control, education tools, single phase systems.

توليد نبض الفولطية العالي

أحمد حسن محمد
جامعة تكريت / كلية الهندسة / قسم الكهرباء
تاريخ استلام البحث:2011/3/29 تاريخ قبول البحث:2013/11/3

الخلاصة

البؤر الورقية على الهندسة اللاكمية الجديدة في مصدر الفولطية عالي لنمط النبض الناتج المتغير ويعرض تعديل مستقل من المقدار والتردد والتكرار والمدة والنبض والتقاطب . المرحلة الكهربائية لمحول المستوى المتعدد تشمل ثمانية مصادر أحادية القطب الفردية التي يمكن ان تكون مرتبِطة إعتباطيا في السلسلة للحصول على نبض فولطية الناتج المطلوب لعدة أمبيرات ومع du/dt عالية جدا .

الكلمات الدالة: مزودات قوة DC ، السيطرة ، الادوات ، محولات قوة الذبذبة العالي، محولات مستوى متعدد نمط – منقول مزودات القوة .

Introduction

The non-linear modulations are commonly used for controlling converters with extremely low power losses in comparison with the linear amplifiers. However, the signals, regulated by these commonly used pulse width modulation techniques [1], present a total harmonic distortion, which is relatively high. Nevertheless, the delta and delta-sigma modulations can be used for converter control [2][3] because these techniques present the characteristic to allow a harmonic distortion extremely low.

Using the following figure (fig.1), we illustrate that a delta modulator structure can be easily implemented for controlling the output current of a power converter.

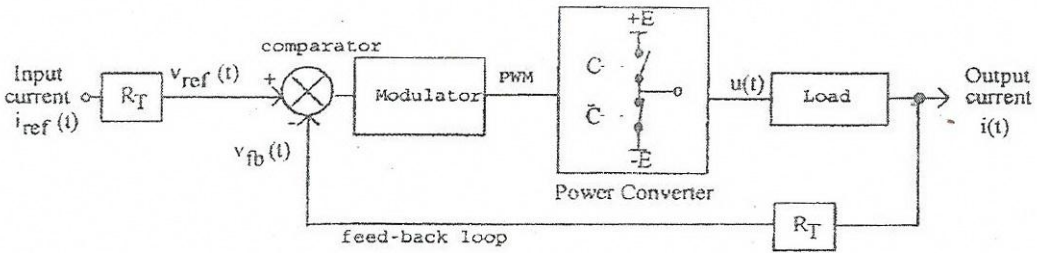

Fig.1 : Principle of the investigated current regulation.

Indeed, the output current goes through an inductive load (R,L), which acts as a first order filter [4]. Thus, in this paper, we demonstrate that such a synoptic matches with a structure involving a delta modulator [5], which is affected by a disturbance.

Delta modulator

Delta modulation principle

As shown by the next figure (fig.2), the delta modulation takes into account the difference $\varepsilon(t)$ between an analog reference signal and a feedback one in order to feed a digital pattern. The sampling is function of a clock whose period equals T_e . thus, the digital output feeds a single bit. There by, this is a one bit analog to digital converter function of booth analog signals. In the feedback loop an integrator smoothes the digital output. In the investigated system, the transfer function of the load acts as an integrator. Therefore, the delta modulator feeds the digital pattern to the power inverter.

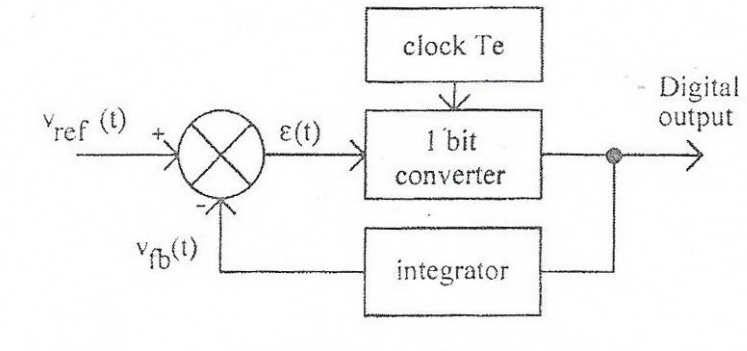

Fig.2: Delta modulation principle.

Investigated system identification

First of all, we choose a constant current reference. Then, the $i_{ref(t)}$ becomes I_{ref} . moreover, the output pulse width modulation signal (whose values equal ±E) is applied to the inductive load (R,L).

As known, the next formula gives the inductive load current :

$$\pm E - R.i(t) = L\frac{di(t)}{dt} \qquad (1)$$

By assuming that the output current accurately tracks the reference current (which us constant) and the output ripple current is negligible, we deduce the following formula :

$$i(t) = \int \frac{\pm E - R.I_{ref}}{L} dt \qquad (2)$$

Thus, we deduce the output current Laplace transform :

$$I(p) = \frac{\pm E - R.I_{ref}}{L_p} \qquad (3)$$

Consequently, the following synoptic (Fig.3) illustrates the previous formula :

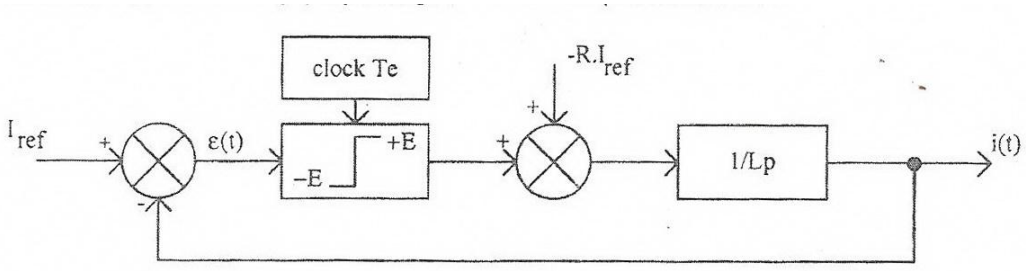

Fig. 3: Theoretical synoptic.

Fig.3: Theoretical synoptic.

By splitting-up the integrator and by moving the inductance coefficient we get the ending synoptic (Fig.4):

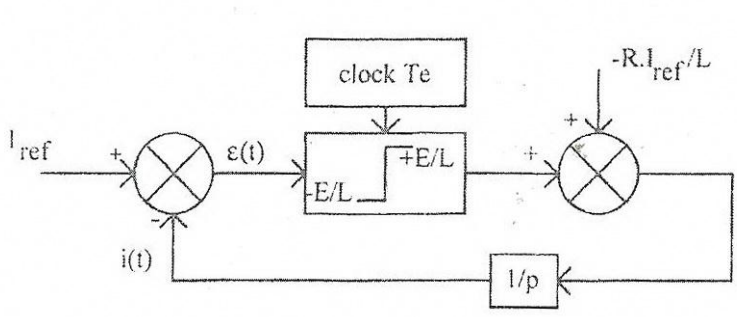

Fig.4: Modified theoretical synoptic.

By viewing this ending synoptic, we illustrate that the system involves a delta modulator with an added disturbance. In the first hand, by assuming the load resistor negligible, then the absolute values of the ripple current slopes values equal. In the other hand, by taking into account the resistor value, the slopes do not equal. Thereafter, the switching events do not

always occur after each sampling event. Thus, the output current spectrum spreads. Such a delta or delta-sigma modulator behavior has been pointed out [6, 7].

Load current spectrum investigations

Varying spectrum in function of a DC reference

Before making analytical investigations, we illustrate that the pulse width frequency of the converter output current (going through the load) changes in function of the DC reference value noted I_{ref} . So, we start by simulating the theoretical system using Matlab-Simulink with the following parameter value:

F_e = 45 kHz	Delta modulation sample frequency
E = 180 V	DC voltage applied on the power converter
L = 27.3 mH	Load inductance (at low frequencies)
R = 4.23Ω	Load resistance
R_T = 1.35 V/A	Sensor current trans-resistance
I_{ref1} = 2.2396A	Reference DC amplitude

Thus, we get the next figure (Fig.5). As shown by viewing the saw teeth of the current ripple, the output current slope sign changes or not after each clock event. If the output current dose not reaches the targeted value, the converter output voltage dose not change. Then the output current slope sign dose not change too, and we have to wait for the next clock event. If the output current reaches the targeted value before the next clock event, the current slope sign changes when the next clock event appears.Regarding the previous results, we can deduce that ripple current frequency changes. Thereby, the reference current modulates the ripple period T.

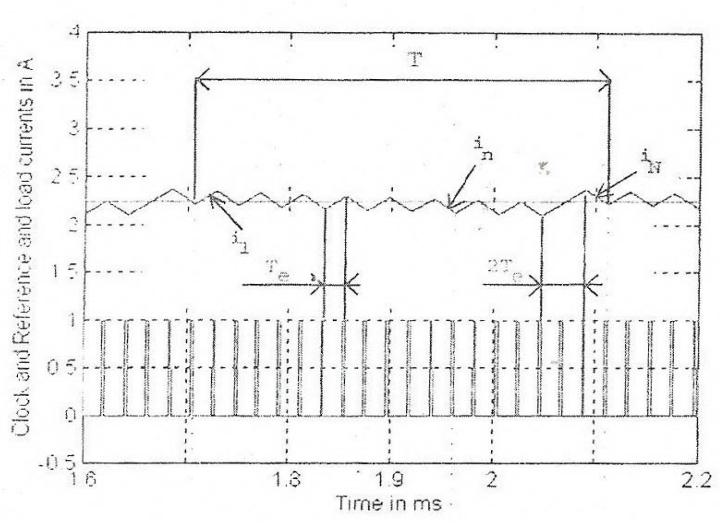

Fig.5: Simulation using the reference current I_{ref} .

As shown by this figure (Fig.5) we assume the output current ripple to be periodic. The period T is equal to the duration between the time events t_0 and t_N . then J_n depicts the current value at the t_n event, and $i_n+I_{(t)}$ depicts the current between the t_n and t_{n+1} events. In short, d_{n+1} defines the duration between the t_{n+1} and t_n events. Moreover, in the followings, m_{n+1}. T_e equals the duration d_{n+1}.

Now, we assume that the following parameter k is equal to the number of the current ripple's saw teeth per period T. This parameter can be link-up with the reference current value I_{ref} .

$i_{n+1}(t)= a (t - t_n) + I_n$ with $a = \frac{+E-R.I_{ref}}{L}$ (positive slope) (4)

$i_{n+2}(t)= b (t - t_{n+1}) + I_{n+1}$ with $b = \frac{-E-R.I_{ref}}{L}$ (negative slope)

Then, considering the current ripple peak value, we get:

$I_{n+1} = a . d_{n+1} + I_n = a . m_{n+1} .T_e + I_n$ (5)

$I_{n+2} = b . d_{n+2} + I_{n+1} = b . m_{n+2} .T_e + I_{n+1}$

Considering a single saw tooth and using the formulas (4) and (5), we deduce the next equation, which indicates if the load current taken as a whole increases or decreases :

$$\frac{I_{n+2} - I_n}{T_e} = \frac{E\,(m_{n+1} - m_{n+2}) - R.I_{ref}\,(m_{n+1} + m_{n+2})}{L} \quad (6)$$

So, considering a positive current reference and the load resistance, we can deduce that the load current decreases (during a whole saw tooth). Thus, in order to make the load current tending to the reference one, the modulator will take into account this variation at the next future sampling events.

Indeed, assuming m_{n+1} and m_{n+2} equal to unity (d_{n+1} equal T_e and d_{n+2} equal T_e), the formula (6) becomes :

$$\frac{I_{n+2} - I_n}{T_e} = \frac{E\,(m_{n+1} - m_{n+2}) - R.I_{ref}\,(m_{n+1} + m_{n+2})}{L} = \frac{-2\,R.I}{L} < 0 \quad (7)$$

During a whole saw tooth, in order to get a positive current variation, the coefficients m_{n+1} and m_{2+2} must not be equal. By keeping m_{n+2} equal to unity (on negative slope), we can look for the positive slop condition :

$E (m_{n+1} - 1) - R.I_{ref} (m_{n+1} +1) > 0$, then : $m_{n+1} > \frac{E+R.I_{ref}}{E-R.I_{ref}} > 1$ (8)

Consequently, during a whole saw tooth and in order to get a positive variation of the load current, the only need is that the m_{n+1} parameter equals two, then d_{n+1} equals $2T_e$. Such a theoretical result can e viewed on the previous figure (Fig.5).

So, we can conclude that the current ripper, whose period equals T, decreases during the first (k-1) saw teeth and the current variation (pre saw tooth) is given by the formula (7). Then, during the ending saw tooth (per period), the current variation is positive, then given by the next simplified formula :

$$\frac{I_{n+2} - I_n}{T_e} = \frac{E\,(m_{n+1} - m_{n+2}) - R.I_{ref}\,(m_{n+1} - m_{n+2})}{L} = \frac{E - 3R.I_{ref}}{L} > 0 \qquad (9)$$

Assuming the current ripple to be periodic (as already done), the total variation $\Delta i(t)$ equals 0. In another way, at the time events t_0 and t_N, the instantaneous load current equals the initial I_0 value.

$$\frac{\Delta i(t)}{T_e} = \frac{I_N - I_0}{T_e} = (k - 1)\frac{-2R.I_{ref}}{L} + \frac{E - 3R.I}{L} = 0 \qquad (10)$$

Thus, we get three equations which link the number k of saw teeth, the period T and the current reference I_{ref} :

$$k = \frac{1}{2}\left(\frac{E}{R.I_{ref}} - 1\right) \text{ or } I_{ref} = \frac{E}{(2k+1)R} \text{ or } I_{ref} = \frac{T_e}{T}\frac{E}{R} \qquad (11)$$

As the current ripple period equals (2k+1). Te, this investigation demonstrates that the period T changes. This is the reason why the load current spectrum spreads. Using the following parameters, E=180 V, R=4.23Ω, I_{ref1}=2.2396A, we get the k value k1=9. This result can be check with the figure (Fig.5). using another current reference value I_{ref2}=3.2733A, then get another k value (k_2=6) and so on.

Spectrum investigations for computation when using an Ac reference signal

Now, in order to look for an analytical mean for computing the current spectrum, first we have to look at the next figure, showing the load current computed using the next parameter :

F_e = 45 kHz	Delta modulation sample frequency
fs = 200 Hz	Input sine wave frequency
E = 180 V	DC voltage applied on the power converter
L = 27.3 Mh	Load inductance (at low frequencies)
R = 4.23Ω	Load resistance
R_T = 1.35 V/A	Sensor current trans-resistance
I = 1A	Input sine wave amplitude

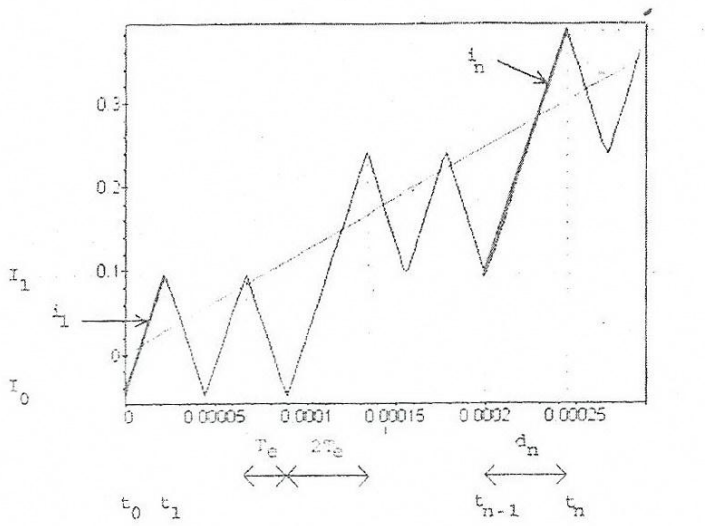

Fig.6: Converter (controlled by delta modulation) output current.

Considering a sine ware reference, once again the load current is made of elementary currents $i_n(t)$ defined between the time events t_{n-1} and t_n as it when using a Dc reference. By summing all these elementary currents, we get the i(t) current, which is defined between 0 and t_N, where t_N is closed to the sine wave reference one.

Now, knowing the practical parameters, it is possible to compute all the $i_n(t)$ time functions and theirs Laplace transformed function $I_n(p)$. By summing the whole elementary Laplace functions, we get the I(p) Laplace one corresponding to the i(t) time function.

Moreover, we compare the Laplace and the Fourier transforms assuming the output current equals 0 before 0s and after t_N. According to the time definitions, we demonstrate that the I(p) Laplace function equals the I(f) Fourier function. Thus we get the Fourier transform of the i(t) current.

Then, assuming that t_N equal Ts (as already assumed), we can get the Fourier transform of the $i_L(t)$ signal defied from $-\infty$ to $+\infty$ (whose period equal Ts). Indeed, by repeating the i(t) time function, we get the $i_L(t)$ one. So, the Fourier coefficients can be defined and the current spectrum can be illustrated.

Thereafter, by using the previous guidelines, we give the followings formulas, which permit to computer the load current spectrum.

Laplace transform of the current i(t)

The inverter output voltage equals ±E. So, we deduce the elementary $u_n(t)$ signals defined between the time events t_{n-1} and tn. Where an equals ±1 and $\Gamma(t)$ is the Heaviside function :

$$u_n(t) = a_n \,.\, E.\, [\Gamma\,(t - t_{n-1}) - \Gamma\,(t - t_n)] \qquad (12)$$

$$= (-1)^{n-1}.\, E.\, [\Gamma\,(t - t_{n-1}) - \Gamma\,(t - t_n)] \quad \text{where } n > 0$$

Thereafter, we deduce the $i_n(t)$ formulas defined between the time events t_{n-1} and t_n, where I_{n-1} are the initial current values :

$$i_n(t) = \left[\frac{a_n.E}{R} - \left(\frac{a_n.E}{R} - I_{n-1}\right)\exp\left(\frac{t - t_{n-1}}{\tau_1}\right)\right] . (\Gamma(t - t_{n-1}) - \Gamma(t - t_n)) \quad (13)$$

$$= \frac{a_n.E}{R}\left[1 - \left(1 - \frac{R.I_{n-1}}{a_n.E}\right)\exp\left(\frac{t - t_{n-1}}{\tau_1}\right)\right] . (\Gamma(t - t_{n-1}) - \Gamma(t - t_n))$$

Considering the whole elementary in(t) signals involved during the sinwave period Ts, we deduce the i(t) signal ending at t_N. Assuming the parameter d_n is equal to the difference between t_n and tn-1, then we can write the following expressions :

$$i(t) = \sum_{n=1}^{N}[\, i_n\,(t - t_{n-1})\,.\,(\Gamma(t - t_{n-1}) - \Gamma(t - t_{n-1} - d_n))] \quad (14)$$

$$= \sum_{n=1}^{N}[\, i_n\,(t)\,.\,(\Gamma(t) - \Gamma(t - d_n))] * \delta(t - t_{n-1})\,]$$

Where $\delta(t\text{-}t_{n-1})$ is another way to define the delay, and δ (t) is the dirac pulse.

So, we deduce the I(p) Laplace transform of the previous i(t) time function :

$$I(p) = L[i(t)] = \sum_{n=1}^{N}[\, L[\, i_n\,(t)\,.\,(\Gamma(t) - \Gamma(t - d_n))]\,.\,L(\delta(t - t_{n-1}))\,] \quad (15)$$

$$I(p) = \sum_{n=1}^{N}[(\int_0^{+\infty} i_n(t).(\Gamma(t) - \Gamma(t - d_n)).\exp(-p1)\,dt\,).(\exp(-p1_{n-1}))]$$

Expending the previous formula, we give a second equation taking into account that the elementary currents in(t) are defined between the time events t_{n-1} and t_n :

$$I(p) = \sum_{n=1}^{N}[(\int_0^{dn} i_n(t)\,.\exp(-p1)\,dt\,).(\exp(-p1_{n-1}))] \quad (16)$$

$$I(p) = \int_0^{I_N} i(t)\,.\exp(-p1)\,dt \quad (17)$$

Fourier transform of the current i(t)

The Fourier transform I(f) of the i(t) signal is given by :

$$I(f) = F[i(t)] = \sum_{n=1}^{N} F[i_n(t).(\Gamma(t) - \Gamma(t - d_n))].\ F[\delta(t - t_{n-1})]$$

$$I(f) = \sum_{n=1}^{N}[(\int_{-\infty}^{+\infty} i_n(t).(\Gamma(t) - \Gamma(t - d_n)).\exp(-2\pi jft)dt)(\exp(-2\pi jft_{n-1}))]$$

$$I(f) = \sum_{n=1}^{N}[(\int_0^{dn} i_n(t).\exp(-2\pi jft)\,dt\,)\,(\exp(-2\pi jft_{n-1}))] \quad (18)$$

$$I(f) = \int_0^{I_N} i(t).\exp(-2\pi jft)\,dt\,) \quad (19)$$

Assuming that p equals 2πjft, then I(p) equals I(f). This permits to link the Laplace and the Fourier transforms .

Fourier transform of the current iL(t)

As already assumed, the signal i(t) is defined between the time events 0 and T_N, where T_N nearly equals T_s. Here we assume that L(t) is equal to the repeated signal i(t) whose period equals T_s. Then, we get its equation :

$$i(t) = i\,(t + T_s) = i_L(t) \Longrightarrow Rep_{T_s}\,[i(t)] \quad (20)$$

Therefore, due to the periodic function $i_L(t)$, the I_k coefficients of Fourier's series can be evaluate by means of the Fourier transform, then by the Laplace transform using the links as previously given :

$$I_k = \frac{1}{T_s}\int_0^{I_N} i_L(t).\exp(-2\pi j f t)\,dt \quad \text{with } f = \frac{k}{T_s} \qquad (21)$$

$$= \frac{1}{T_s}\int_0^{I_N} i_L(t).\exp(-2\pi j \frac{k}{T_s} t)\,dt \quad \text{with } t_N \approx T_s$$

Due to the equations (17) and (19), we deduce :

$$I_k = \frac{1}{T_s}.\, I(p) \text{ with } p = 2\pi j f \text{ and } f = \frac{k}{T_s} \qquad (22)$$

$$I_k = \frac{1}{T_s}.\, I(f) \text{ with } f = \frac{k}{T_s}$$

Fourier series coefficients of the current iL(t)

Furthermore, considering these periodic $i_L(t)$ function, the Fourier series verify the next formulas [8] :

$$i_L(t)=\sum_{k=-\infty}^{+\infty} I_k \exp(2\pi j \frac{k}{T_s} t)=I_0 +\sum_{k=1}^{+\infty}[\, I \exp(2\pi j \frac{k}{T_s} t)+ I_{-k} \exp(2\pi j \frac{k}{T_s} t)] \quad (23)$$

$$i_L(t)=C_0 + \sum_{k=1}^{+\infty} C_k \cos(2\pi \frac{k}{T_s} t + \varphi_k) \text{ with } C0 = I_0 \text{ and } C_k = 2\,|I_k|$$

Thus, we find the ending formula necessary for spectrum computation :

$$C_k = 2\left|\frac{1}{T_s} I\left(\frac{k}{T_s}\right)\right| = 2\left|f_s I\left(\frac{k}{T_s}\right)\right| = 2f_s\sqrt{\Re^2\left(I_N\left(\frac{k}{T_s}\right)\right) + \Im^2\left(I_N\left(\frac{k}{T_s}\right)\right)} \quad (24)$$

Computed spectrum

In order to get some load current spectrum plots, we use the Maple V software. So, the compilation involves the given computation process which links the Fourier series, the Fourier transform and the Laplace transform. The following figure (Fig.7) illustrates two of the plots :

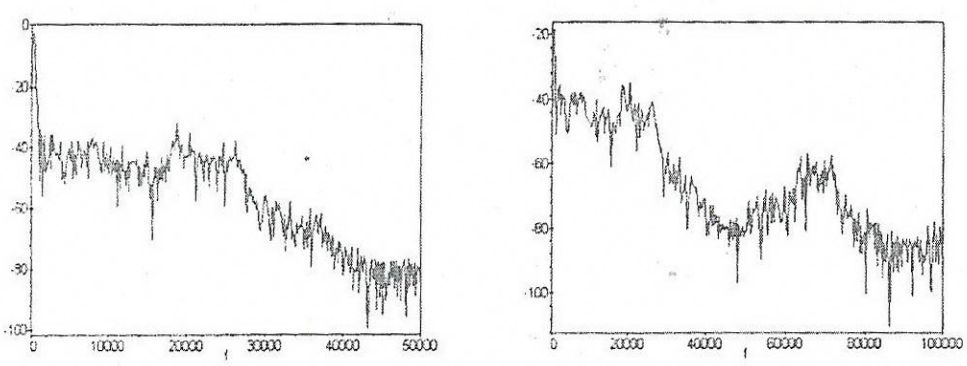

Fig.7: Computed load current spectrums (using Maple V).

Considering two bandwidths (50kHz and 100kHz), we can see the main prominent line whose frequency equals 200 Hz. Then, in a bandwidth going from 0Hz to 30kHz, the intermediation line amplitudes are bound around -30dB, showing the low THD in case of power electronic applications. Furthermore, we can clearly see the notches. They are located around 45kHz and 90kHz (the multiples of the delta modulation sampling frequency F_e). This confirms the presence of notches as previously pointed out. These plots also check the way to compute the spectrum.

Simulated results according to the simplified delta modulator board

The simulations takes into account a simplified board which always keeps additional filters, involved in the whole board, used for noise reduction. Then, for simulation (using Matlab-simulink), the parameter value are given by :

F_e = 45 kHz	Delta modulation sample frequency
fs = 200 Hz	Input sine wave frequency
E = 180 V	DC voltage applied on the power converter
L = 27.3 Mh	Load inductance (at low frequencies)
R = 4.23Ω	Load resistance
R_T = 1.35 V/A	Sensor current trans-resistance
I = 1A	Input sine wave amplitude

By looking at the next figure (Fig.8) we can see the output current going through the load. It well tracks the sineware reference whose frequency equals 200Hz. It can be noticed that the output current ripples change. Thus, this phenomenon characterizes the delta pulse width modulation technique as described in the previous theoretical analysis.

As shown with one of the figures (Fig.7),the previous figure (Fig.9) illustrates the spectrum density of the output current. We can see the main prominent line whose frequency equals 200Hz and its relative amplitude, which equals 0 dB. Then, using the same bandwidth going from 0Hz to 30kHz, the intermediation line amplitudes are bound around -30dB. As already described, notches are located around 4.5kHz and 90kHz accordingly to the theoretical investigations and spectrum computations (Fig.7). Simulated spectrums look very similar to the computed once. Thus, this result checks and validates the investigated spectrum analysis when the reference is a sinus wave.

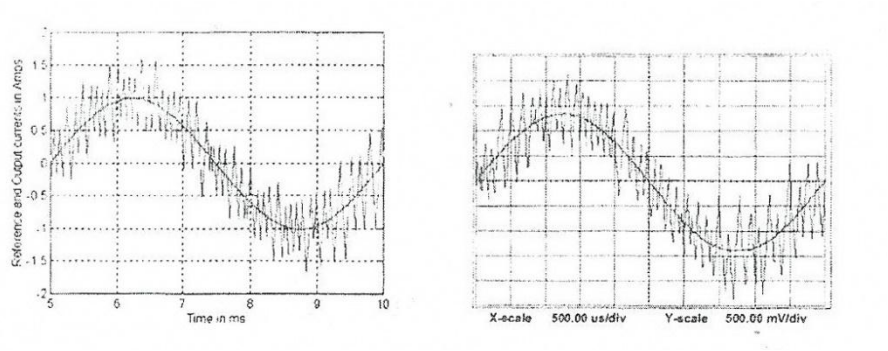

Fig.8: Input $i_{ref}(t)$ and output i(t) currents simulations (using Matlab-Simulink).

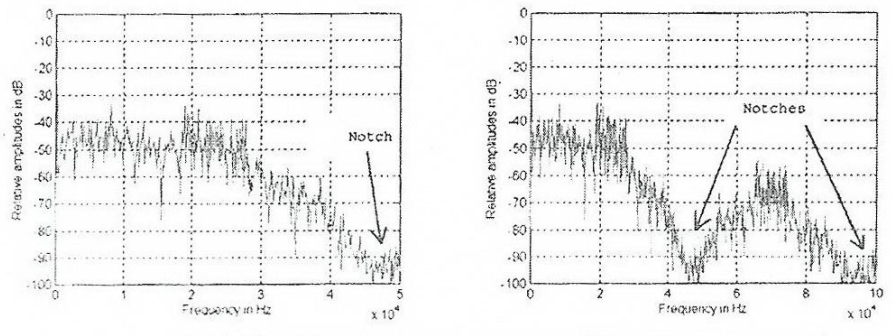

Fig.9: Simulated load current spectrums (using Matlab-Simulin)

Experiments and simulations comparisons

Simplified delta modulator board and whole system

The next figure (Fig.10) illustrates the whole system for research and student investigations :

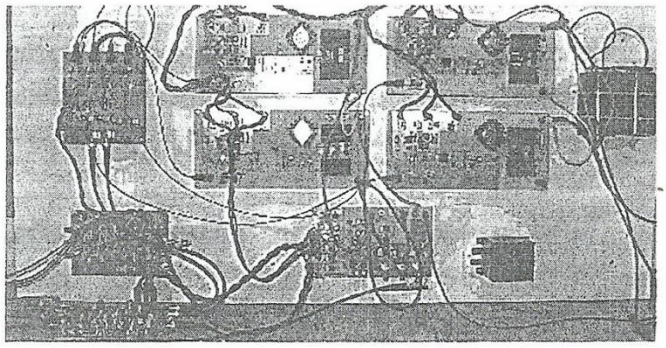

Fig.10: Modular system for research and student investigations.

The delta modulator board implements a filter whose transfer function is F(p). This filter, located after the error detector, is used for reducing the bandwidth and the static error as it is when using anther pulse modulation technique [9][10][11]. So, it is an added filter in comparison with the basic delta modulation synoptic. The filtered error is sampled and held using a tuning clock whose period is T_e. By means of a one-bit analogue to digital converter (in fact a comparator), we finally get the pulse width modulated signal and its opposite.

Which are applied to the power switches through optical link. Thus, there is a great electrical isolation between the modulation and the inverter in order to increase the quality of the measurements. This previous isolation is not shown on the system synoptic.

In fact, the whole power converter is built involving few boards (Fig.10) in order to get a flexible system, which is used for research and student investigations on pulse width modulation techniques and power switches developments. So, the PWM modulator, the isolation board, the power switches and the current sensor board are separately built.

Sine wave reference tracking

For simulation (using Matlab-Simulink) and for experiments, the parameter values are given by :

F_e = 45 kHz	Delta modulation sample frequency
fs = 200 Hz	Input sine wave frequency
E = 180 V	DC voltage applied on the power converter
L = 27.3 mH	Load inductance (at low frequencies)
L = 10.2 mH	Load resistance (at 45 kHz)
R = 4.23Ω	Load resistance
R_T = 1.35 V/A	Sensor current trans-resistance
I = 1A	Input sine wave amplitude

In order to compare the experimental spectrum shapes with the theoretical ones (Fig.7), we choose a current reference whose peak equals one Amp, even if it is possible to apply 3 Amps peak to the load. First of all, we compare the simulated load current (using a complex board) with the current that we get by measurements (Fig.11). It can be viewed that the ripple variations are very similar. For information, by increasing the current reference amplitude (or decreasing the E value), the ripple decreases.

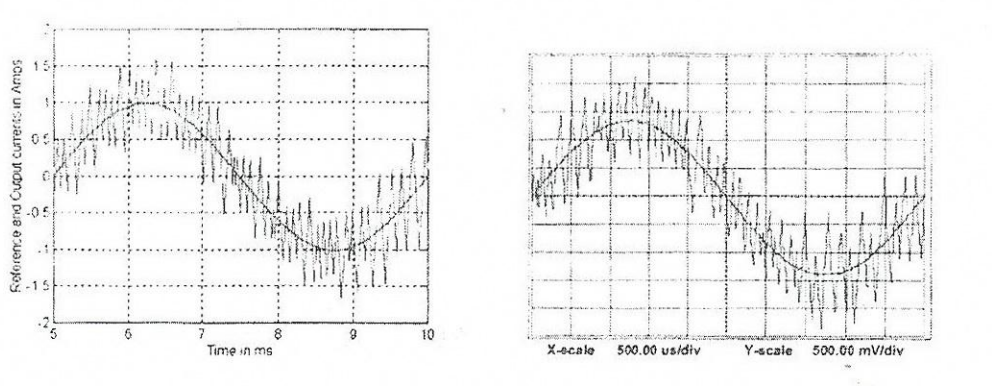

Fig.11: Simulated and experimental reference and load currents.

Now, the following figure (Fig.12) shows the simulated and experimental current spectrums. Both spectrums also are very similar. We can see the first notch (around 45kHz) by simulating. This in not viewed on the experimental plot due to the bench measurement specifications, Considering a bandwidth going from 0 to 10khz, the inter modulation line amplitudes are bound to -20dB in both cases. For information, targeting a 3 Amps peak current, this value decreases to -30dB.

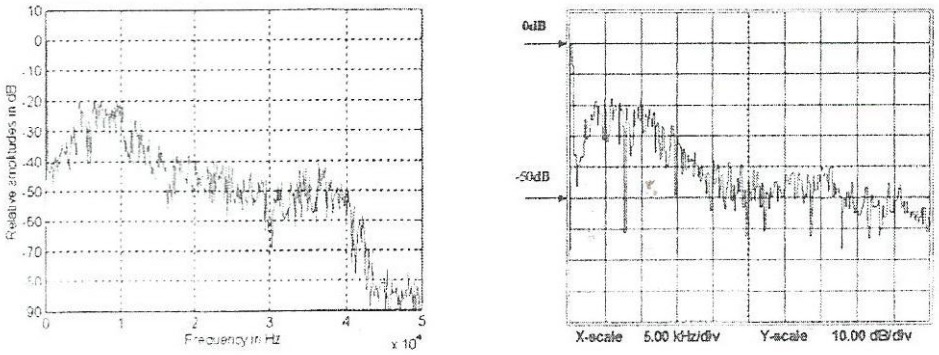

Fig.12: Simulated and experimental load current spectrums.

Conclusion

Here, we investigate the delta modulation. A board implements this modulation technique in order to control the power converter output current. As the load is inductive, we demonstrate that the investigated structure matches with a delta modulation with an added disturbance. By means of theoretical investigations involving the Laplace and Fourier transforms, we demonstrate that it is possible to get the current spectrum which is spread and presents notches around the multiples of the sampling period. Furthermore, the whole system is designed for modularity. So, students can do experiments with theirs own modular boards for investigating modulation techniques or power devices.

References

[1] J. HOLTZ, Pulse width Modulation – A Survey, IEEE Trans. Indus, Elec, Vol.39, December 1992, N5, PP.410-420 .

[2] E. DALLAGO, G. SASSONE, Advance in High-Frequency Power Conversion by Delta-Sigma Modulation, IEEE Trans. Circuits Syst., Vol.44, August 1997, N8, PP.712-721.

[3] A.J. FRAZIER, M.K. KSZIMIERCZUK, DC-AC Power Inversion Using a-b Modulation, IEEE Trans Circuits Syst., Part1, Vol47, January 2000, N1, PP.79-82.

[4] K.M. SMEDLEY, : Integrators in Pulse Width Modulation, IEEE Power Electronic Specialists Conference, June 1996, PP.773-781 .

[5] P.F. PANTER : Modulation. Noise and Spectral Analysis, Mc Graw Hill Book Company Inc., New York, USA, 1965.

[6] T.C GREEN, Spectra of delta-Sigma Modulated Inverters : As Analytical Treatment, IEEE Trans Power Elect., Vol.7, October 1992, N4, PP.644-654.

[7] H.E. ROWE, Signals and Noise in Communication System, D. Van Nostrand Company Inc., Princeton, New Gersey, USA, 1965.

[8] F. AUGER, Introduction ala theorie du signal et de information, Collection Sciences et Technologies, Editions Technip, Paris, France, 1988.

[9] J.C. LE CLAIRE, S. SIALA, J. SAILLARD, R. LE DOEUFF, A new Pulse Modulation for Voltage Supply Inverter's Current Control, 8th European Conference on Power Electronics and Applications Lausanne, Switzerland, September 1999, CD-ROM ref1SBN 90-75815-04-2 .

[10] J.C. LE CLAIRE, S. SIALA, J. SAILLLARD, R. LE DOEUFF, A Resonant Current Controller far fast AC Voltage Regulation, 8th International Conference on Power Electronic and Variable Speed Drives, London, United Kingdom, September 2000, PP.305-310.

[11] J.C. LE CLAIRE, A new Resonant Voltage Controller far fast AC Voltage Regulation of a Single-Phase DC/AC Power Converter, Power Conversion Conference, Osaka, Japan, April 2002, PP.1067-1072.